Author Manuscript

Author Manuscript

Author Manuscript

Author Manuscript

HHS Public Access

Author manuscript

Angew Chem Int Ed Engl. Author manuscript; available in PMC 2024 April 17.

Published in final edited form as:

Angew Chem Int Ed Engl. 2023 April 17; 62(17): e202218175. doi:10.1002/anie.202218175.

Reactivities of α-Oxo BMIDA Gold Carbenes Generated by Gold-Catalyzed Oxidation of BMIDA-Terminated Alkynes

Yang Zheng[a],‡, **Jingxing Jiang**[c],‡, **Yue Li**[a], **Yongliang Wei**[a], **Junqi Zhang**[a], **Jundie Hu**[d], **Zhuofeng Ke**[c], **Xinfang Xu**[b], **Liming Zhang**[a]

[a]Department of Chemistry and Biochemistry, University of California, Santa Barbara, CA 93106, USA

[b]School of Pharmaceutical Sciences, Sun Yat-sen University, Guangzhou 510006, P. R. China

[c]School of Materials Science & Engineering, PCFM Lab, Sun Yat-sen University, Guangzhou 510275, P. R. China

[d]School of Materials Science and Engineering, Suzhou University of Science and Technology, Suzhou, 215009, P. R. China

Abstract

An oxidative strategy is reported to access α-oxo BMIDA gold carbenes directly from BMIDA-terminated alkynes. Besides offering expedient access to seldom studied boryl metal carbenes, these BMIDA gold carbene species undergo facile insertions into methylene, methine, and benzylic C-H bonds in the absence of the Thorpe-Ingold effect. They also undergo efficient OH insertion, cyclopropanation, and F-C alkylations. This chemistry provides rapid access to structurally diverse α-BMIDA ketones, which are scarcely documented. In combination with DFT studies, the role of BMIDA is established to be an electron-donating group that attenuates the high electrophilicity of the gold carbene center.

Graphical abstract

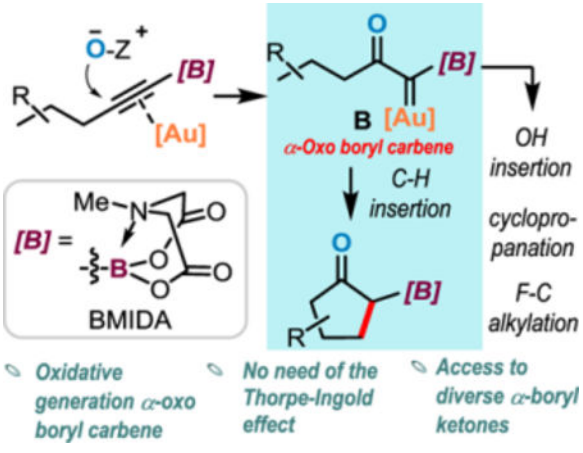

zhang@chem.ucsb.edu .

‡These authors contribute equally.

Author Manuscript Author Manuscript Author Manuscript Author Manuscript

α-Oxo BMIDA gold carbenes are oxidatively generated from BMIDA-terminated alkynes. With the electrophilicity modulated by BMIDA, these carbene species undergo C-H insertion in the absence of the Thorpe-Ingold effect. This chemistry provides expedient access to structurally diverse α-boryl ketones, which are scarcely documented.

Keywords

alkynes; α-boryl ketones; carbenes; C–H insertion; gold catalysis

Gold-catalyzed oxidation of alkyne by an external nucleophilic oxidant[1] has offered a versatile strategy for methodology development since the original report in 2010.[2] In comparison to the dediazotization approach,[3] it constitutes safe and expedient access to a variety of α-oxo gold carbene intermediates or their reactivity equivalents of exceptional reactivities from a range of functionalized precursors (Scheme 1A). To date, various types of α-*oxo* gold carbene species including α-*oxo* terminal gold carbene,[2, 4] 1,3-dicarbonyl gold carbenes,[5] donor/acyl-substituted gold carbenes,[6] amido gold carbenes,[7] and silyl/acyl gold carbenes (**A**)[8] have been generated or proposed as key reaction intermediates by using benign and readily available alkynes instead of diazo carbonyl compounds as substrates. The substitutions at the gold carbene center play essential roles in modulating its reactivities and facilitating versatile transformations. For example, the silyl substitution in the gold carbene **A** dictates the Wolff rearrangement as the predominant reaction pathway.

α-Boryl diazo compounds including those possessing an α-acyl moiety are known, and examples are shown in the left column of Scheme 1B.[9] No organic transformations of these compounds have been documented, let alone their metal-promoted/catalyzed formation of boryl metal carbene intermediates. An exception was not reported until 2021. In this work by Liu and co-workers,[10] stable 1-TBS-2-diazomethyl-1,2-azaborine (TBS: *t*-butyldimethylsilyl) engages in a range of reactions including Ru-catalyzed carbonyl olefination and $Rh_2(OAc)_4$-catalyzed intramolecular insertion into unactivated C-H bonds (Scheme 1b, right column). In the Ru catalysis, a boryl Ru carbene intermediate was isolated and shown to be catalytically competent.

To push the frontier of oxidative gold catalysis and introduce new entries to the much-underexplored boryl metal carbene chemistry, we envisioned that an α-*oxo* boryl gold carbene of type **B** could be oxidatively generated from a BMIDA-terminated alkyne in the presence of a suitable nucleophilic oxidant (Scheme 1C). Herein, we report a successful implementation of the strategy and disclose the reactivities of the α-*oxo* BMIDA gold carbenes and in particular their extraordinary C-H insertion chemistry[11] *via* a combination of experimental studies and DFT calculations.

At the outset, we employed 1-BMIDA-oct-1-yne (**1a**) as the model substrate for reaction discovery and conditions optimization. To our delight, in the presence of $IPrAuNTf_2$ (5.0 mol %) as the catalyst and 8-isopropylquinoline *N*-oxide (**2a**) as the oxidant,[12] the desired C-H insertion product **3a** was obtained in 80% yield when the reaction was performed in $PhCF_3$ at 60 °C for 10 h (entry 1, Table 1). The diastereomeric ratio of **3a** is >20:1, and the *trans* configuration of the major product isomer is corroborated by the XRD structure of

Author Manuscript Author Manuscript Author Manuscript Author Manuscript

5 (*vide infra*). What is remarkable is that in this reaction the C-H insertion by the putative α-*oxo* BMIDA gold carbene occurred with high efficiency in the absence of the Thorpe-Ingold effect, which is indispensable in our previous gold carbene C-H insertion chemistry.[5f, 13] Additional catalysts including $IMesAuNTf_2$, $IPr^{Me}AuCl/AgNTf_2$, $MorDalPhosAuNTf_2$, $Me_4tBuXPhosAuCl/AgSbF_6$, $IPrAuCl/AgSbF_6$, and $AgNTf_2$ were also investigated but did not lead to improved results (entries 2–7). While the use of 8-methylquinoline *N*-oxide (**2b**) resulted in a lower yield of **3a** (entry 8), those oxidants derived from pyridines, however, were completely ineffective (entries 9 and 10). Other solvents including DCE, PhF, toluene, and THF were less effective or not suitable (entries 11–14).

With the optimal reaction conditions in hand, we first explored the scope of insertion into methylene C-H bonds. As shown in Table 2, substrates containing nonfunctionalized alkyl chains (entries 1–2) or functionalized ones (entries 3–4) reacted smoothly to deliver the α-BMIDA cyclopentanone products **3a**-**3d** in good yields. The insertion into cyclohexane C-H bonds also worked, affording trans-fused **3e** as the major isomer (entry 5). The relative configuration of **3e** is confirmed in the studies shown in Scheme 2 (*vide infra*). In addition, a cyclopropyl group α to the carbonyl group of the product **3f** was tolerated (entry 6). Next, we investigated the insertions into more reactive C(sp^3)-H bonds, including primary and secondary benzyl C(sp^3)−H bonds, and a tertiary C(sp^3)−H bond. Remarkably, these reactions proceeded without incident to generate the desired C-H insertion products efficiently (entries 7–9). Even more so is the smooth insertion into an unactivated methyl group, affording the parent α-BMIDA cyclopentanone **3j** in 67% yield (entry 10). To explore the synthetic utility of this C-H insertion chemistry, the substrate **1k** derived from (*S*)-citronellol was subjected to the C-H insertion chemistry, which was followed by protodeboronation upon the treatment with NaOH in a mixed solvent of tetrahydrofuran and water (entry 10). The cyclopentanone product **3k'** featuring an all-carbon quaternary chiral center was isolated in 70% overall yield with excellent enantiomeric excess (96%). This two-step protocol permits BMIDA to behave as a traceless facilitating group and formally realizes a concerted C-H insertion by a terminal α-oxo gold carbene, which owing to its high reactivity does not undergo selective C-H insertion.

DFT calculations were performed to elucidate the mechanism of this unusually effective C-H insertion. The reaction free energy profile is illustrated in Figure 1. The gold-alkyne complex **RC** is attacked by the *N*-oxide **2a** to form an intermediate **IM1** (5.8 kcal/mol) *via* the transition state **TS1** with a calculated free energy of 13.7 kcal/mol. Subsequently, an N-O bond cleavage leads to the dissociation of 8-isopropylquinoline from **IM1** *via* transition state **TS2** (19.3 kcal/mol), generating the α-oxo BMIDA gold carbene **IM2** (−18.6 kcal/mol). A conformation change of **IM2** to **IM2'** (−18.1 kcal/mol) leads to the formation of the agostic intermediate **IM3** (−20.9 kcal/mol) *via* the transition state **TS3** (−18.1 kcal/mol). **IM3** then undergoes a surprisingly facile C-H insertion *via* the transition state **TS4**, with an activation free energy of only 1.9 kcal/mol. In comparison, the transition states leading to a cyclobutanone[5f, 13] and ketene/1-butene[5f] are calculated to be 1.8 and 4.7 kcal/mol higher in free energy than **TS4**, respectively (Figure S1), consistent with the lack of these side reactions.

Author Manuscript Author Manuscript Author Manuscript Author Manuscript

To understand the essential role of the BMIDA moiety in facilitating efficient C-H insertion, we investigated computationally the C-H insertion step with it replaced by a methyl group or a benzoyl group. The former is known to lead to 1,2-C-H insertion to form enones,[12], and the latter results in C-H insertions with the assistance of the Thorpe-Ingold effect.[5f, 13] As shown in Figure 2, electronic structure analysis shows that the BMIDA substituted carbene **IM2** has a lower LUMO energy (−6.34 eV) than that of the Me substituted carbene **IM2-Me** (−6.28 eV) or the Bz substituted carbene **IM2-Bz** (−6.06 eV). As these LUMOs have large coefficients on the carbene centers, their energy levels reflect the relative electrophilicity and hence reactivities of the carbene centers, with that of **IM2** being the least electrophilic and that of **IM2-Bz** the most electrophilic of the three. This consideration is consistent with Bz being electron-withdrawing and methyl electron-donating, and suggests that BMIDA is slightly more electron-donating than Me. Moreover, Fukui Functions also suggest a decreased electrophilicity of the α-oxo BMIDA gold carbene center (0.210) (Table S1), which is in line with BMIDA being more electron-donating than a methyl group. These results are consistent with that the BMIDA gold carbenes generated in this work exhibit attenuated and hence more chemoselective C-H insertion reactivities. As such, the Thorpe-Ingold effect is not required to avoid competing side reactions. Although BMIDA behaves as an electron-withdrawing group in the Wacker oxidation,[14] its electron-donating characteristics in this chemistry are attributed to its tetra-coordination and the high electrophilicity of the carbene center. In contrast, tri-coordinated boryl moieties such as those shown in Scheme 1B exhibit electron-withdrawing characteristics. In addition, it is notable that BMIDA is readily removable, can serve as a valuable functional handle, and unlike alkyl groups that engage in facile 1,2-C-H insertion,[12] does not react with the carbene center.

The Gibbs free energies of the subsequent C-H insertion of **IM2-Me** and **IM2-Bz** were calculated (Figure S2). The barriers leading to cyclopentanone products are 7.6 kcal/mol for **IM2-Me** and 6.5 kcal/mol for **IM2-Bz**. Both are substantially higher than that of the **IM2** (1.9 kcal/mol). Due to the hyperconjugation between its α-methyl C-H bonds, **IM2-Me** does not form the agostic counterpart of **IM3**, which can be seen from the structure and the LUMOs of **IM2'-Me** in Figure S3. In the reaction of **IM2-Bz**, due to the electron-withdrawing Bz group, it has to overcome a barrier of hydride transfer ($\Delta G^{\ddagger}$ = 6.5 kcal/mol) before the C-H insertion (Figure S2).

Author Manuscript Author Manuscript Author Manuscript Author Manuscript

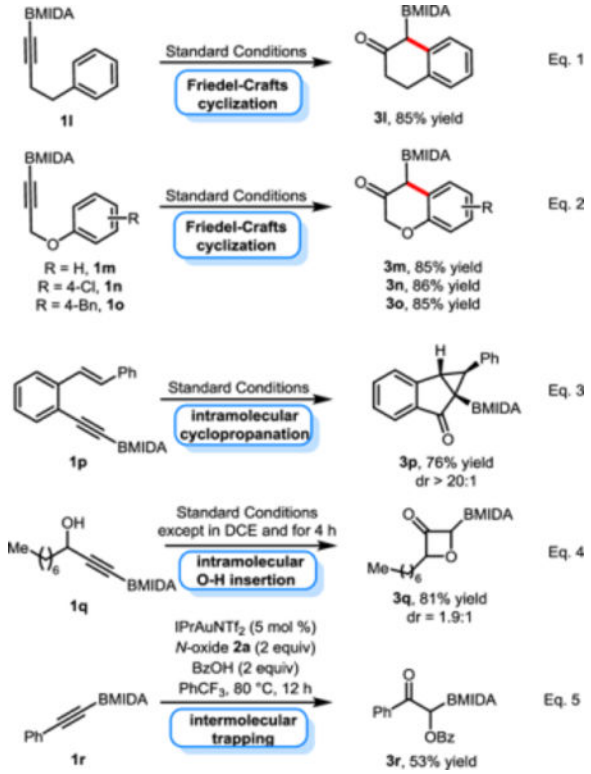

We further explored additional reactivities of the in-situ formed α-*oxo* BMIDA gold carbene intermediate. For example, its intramolecular Friedel-Crafts cyclizations exhibited excellent efficiencies, affording 1-BMIDA-dihydronaphthalen-2-one (**3l**, Eq. 1) and the 4-BMIDA-chroman-3-ones **3m-3o** (Eq. 2) in good to excellent yields. It undergoes facile intramolecular cyclopropanation to afford the tricyclic α-BMIDA indanone **3p** in 76% yield (Eq. 3). Its intramolecular insertion into an O-H bond[5a] is demonstrated in Eq. 4, in which the strained borylated oxetan-3-ones **3p** is formed in 81% yield (dr = 1.9:1). Finally, it was trapped by benzoic acid to afford the functionalized acetophenone product **3r** in a moderate yield (Eq. 5).

While α-BMIDA aldehydes[15] were known as versatile building blocks in organic synthesis, the synthesis of α-BMIDA ketones was only reported once,[14] and their further transformations were not documented. This oxidative gold catalysis provides expedient access to various α-BMIDA ketones of different structural types. To study their synthetic transformations, **3e** was prepared in a gram scale under the optimized reaction conditions, and the scale-up yield remains to be good (Scheme 2A). As in the case of **1k**, the BMIDA group of **3e** was readily removed, albeit under acidic conditions, to afford the volatile bicyclic ketone **4** in 95% NMR yield (Scheme 2B). The *trans* ring fusion of **4** is assigned based on literature reports[16] and confirmed by the following reaction. As shown in Scheme 2C, we subjected **3e** to the Wittig reaction by using pre-generated methylene triphenylphosphorane. Instead of the anticipated methylenation of its ketone group, surprisingly one of the BMIDA ester carbonyl groups undergoes the Wittig reaction and a subsequent double bond isomerization to afford the compound **5** in 70% isolated yield. The structure of **5** is unambiguously established by X-ray diffraction studies and

Author Manuscript Author Manuscript Author Manuscript Author Manuscript

further confirms the 5,6-*trans* ring fusion in **3e**.[17] Notably, we could not find any literature precedent of this transformation. In addition, **3l** was converted regioselectively to the non-conjugated silyl enol ether **6** under kinetic control in 92% yield (Scheme 2D).

In summary, we developed an oxidative strategy to access α-*oxo* BMIDA gold carbenes directly from BMIDA-terminated alkynes. Boryl metal carbenes are seldom studied or invoked in synthetic chemistry, and this BMIDA gold variant undergoes versatile and efficient insertions into methylene, methine, and benzylic C-H bonds in the absence of the Thorpe-Ingold effect, which is indispensable in previously gold carbene C-H insertion reactions.[5f, 13] The ready removal of BMIDA under either basic or acidic conditions formally realizes C-H insertions by terminal α-oxo gold carbenes, which is not attainable due to their high reactivities. In combination with DFT studies, the role of BMIDA is established to be an electron-donating group that attenuates the high electrophilicity of the gold carbene center. The boryl carbene species also undergo efficient OH insertion, cyclopropanation, and F-C alkylation. This oxidative gold catalysis provides expedient access to structurally diverse α-BMIDA ketones, which are scarcely documented.

Supplementary Material

Refer to Web version on PubMed Central for supplementary material.

Acknowledgments

L.Z. thanks NIH (R01GM123342 and R35GM139640) for financial support. Y.Z. thanks the China Scholarship Council for a scholarship and the China Postdoctoral Science Foundation (2021M693279).

References

[1]. (a) Zheng Z, Ma X, Cheng X, Zhao K, Gutman K, Li T, Zhang L, Chem. Rev 2021, 121, 8979–9038; [PubMed: 33591722] (b)Xiao J, Li X, Angew. Chem., Int. Ed 2011, 50, 7226 – 7236;(c)Zhang L, Acc. Chem. Res 2014, 47, 877–888. [PubMed: 24428596] (d)Bhunia S, Ghosh P, Patra SR, Adv. Synth.Catal 2020, 362, 3664–3708.

[2]. Ye L, Cui L, Zhang G, Zhang L, J. Am. Chem. Soc 2010, 132, 3258–3259. [PubMed: 20166668]

[3]. (a) Liu L, Zhang J, Chem. Soc. Rev 2016, 45, 506–516; [PubMed: 26658761] (b)Doyle MP, McKervey MA, Ye T, Modern catalytic methods for organic synthesis with diazo compounds: from cyclopropanes to ylides, Wiley, New York, 1998;(c)Ford A, Miel H, Ring A, Slattery CN, Maguire AR, McKervey MA, Chem. Rev 2015, 115, 9981–10080. [PubMed: 26284754]

[4]. (a) Cai J, Wang X, Qian Y, Qiu L, Hu W, Xu X, Org. Lett 2019, 21, 369–372; [PubMed: 30596509] (b)Karad SN, Liu R-S, Angew. Chem., Int. Ed 2014, 53, 5444–5448;(c)Zeng X, Liu S, Shi Z, Liu G, Xu B, Angew. Chem., Int. Ed 2016, 55, 10032–10036;(d)Yang J-M, Zhao Y-T, Li Z-Q, Gu X-S, Zhu S-F, Zhou Q-L, ACS Catal 2018, 8, 7351–7355.

[5]. (a) Ye L, He W, Zhang L, Angew. Chem., Int. Ed 2011, 50, 3236–3239;(b)Fu J, Shang H, Wang Z, Chang L, Shao W, Yang Z, Tang Y, Angew. Chem., Int. Ed 2013, 52, 4198–4202;(c)Xu Y, Wang Q, Wu Y, Zeng Z, Rudolph M, Hashmi ASK, Adv. Synth. Catal 2019, 361, 2309–2314;(d)Ji K, Yang F, Gao S, Tang J, Gao J, Chem. Eur. J 2016, 22, 10225–10229; [PubMed: 27276524] (e)Qian D, Zhang J, Chem. Commun 2011, 47, 11152–11154;(f)Wang Y, Zheng Z, Zhang L, J. Am. Chem. Soc 2015, 137, 5316–5319. [PubMed: 25835372]

[6]. Chen H, Zhang L, Angew. Chem., Int. Ed 2015, 54, 11775–11779.

[7]. (a) Vasu D, Hung H-H, Bhunia S, Gawade SA, Das A, Liu R-S, Angew. Chem., Int. Ed 2011, 50, 6911–6914;(b)Dos Santos M, Davies PW, Chem. Commun 2014, 50, 6001–6004;(c)Li L, Shu C,

Author Manuscript Author Manuscript Author Manuscript Author Manuscript

Zhou B, Yu Y-F, Xiao X-Y, Ye L-W, Chem. Sci 2014, 5, 4057–4064;(d)Lin M, Zhu L, Xia J, Yu Y, Chen J, Mao Z, Huang X, Adv. Synth. Catal 2018, 360, 2280–2284.

[8]. Zheng Y, Zhang J, Cheng X, Xu X, Zhang L, Angew. Chem. Int. Ed 2019, 58, 5241–5245.

[9]. (a) Schöllkopf U, Bánhidai B, Frasnelli H, Meyer R, Beckhaus H, Justus Liebigs Ann. Chem 1974, 1974, 1767–1783;(b)Arthur MP, Baceiredo A, Bertrand G, J. Am. Chem. Soc 1991, 113, 5856–5857;(c)Sotiropoulos J-M, Baceiredo A, von Locquenghien KH, Dahan F, Bertrand G, Angew. Chem., Int. Ed 1991, 30, 1154–1156;(d)Ansorge A, Brauer DJ, Bürger H, Hagen T, Pawelke G, Angew. Chem., Int. Ed 1993, 32, 384–385;(e)Weber L, Wartig HB, Stammler H-G, Neumann B, Organometallics 2001, 20, 5248–5250.

[10]. Liu Y, Puig R Bellacasa de la, Li B, Cuenca AB, Liu S-Y, J. Am. Chem. Soc 2021, 143, 14059–14064. [PubMed: 34431676]

[11]. Doyle MP, Duffy R, Ratnikov M, Zhou L, Chem. Rev 2010, 110, 704–724. [PubMed: 19785457]

[12]. Lu B, Li C, Zhang L, J. Am. Chem. Soc 2010, 132, 14070–14072. [PubMed: 20853846]

[13]. Zheng Z, Wang Y, Ma X, Li Y, Zhang L, Angew. Chem. Int. Ed 2020, 59, 17398–17402.

[14]. Corless VB, Holownia A, Foy H, Mendoza-Sanchez R, Adachi S, Dudding T, Yudin AK, Org. Lett 2018, 20, 5300–5303. [PubMed: 30129366]

[15]. (a) Soor HS, Diaz DB, Burton KI, Yudin AK, Angew. Chem., Int. Ed 2021, 60, 16366–16371; (b)Lee CF, Diaz DB, Holownia A, Kaldas SJ, Liew SK, Garrett GE, Dudding T, Yudin AK, Nature Chemistry 2018, 10, 1062–1070;(c)He Z, Zajdlik A, Yudin AK, Acc. Chem. Res 2014, 47, 1029–1040. [PubMed: 24495255]

[16]. (a) Kirschberg T, Mattay J, J. Org. Chem 1996, 61, 8885–8896; [PubMed: 11667869] (b)Wei Y, Rao B, Cong X, Zeng X, J. Am. Chem. Soc 2015, 137, 9250–9253. [PubMed: 26172049]

[17]. Deposition Number 2219760 (5) contains the supplementary crystallographic data for this paper. These data are provided free of charge by the joint Cambridge Crystallographic Data Centre and Fachinformationszentrum Karlsruhe Access Structures service.

Author Manuscript Author Manuscript Author Manuscript Author Manuscript

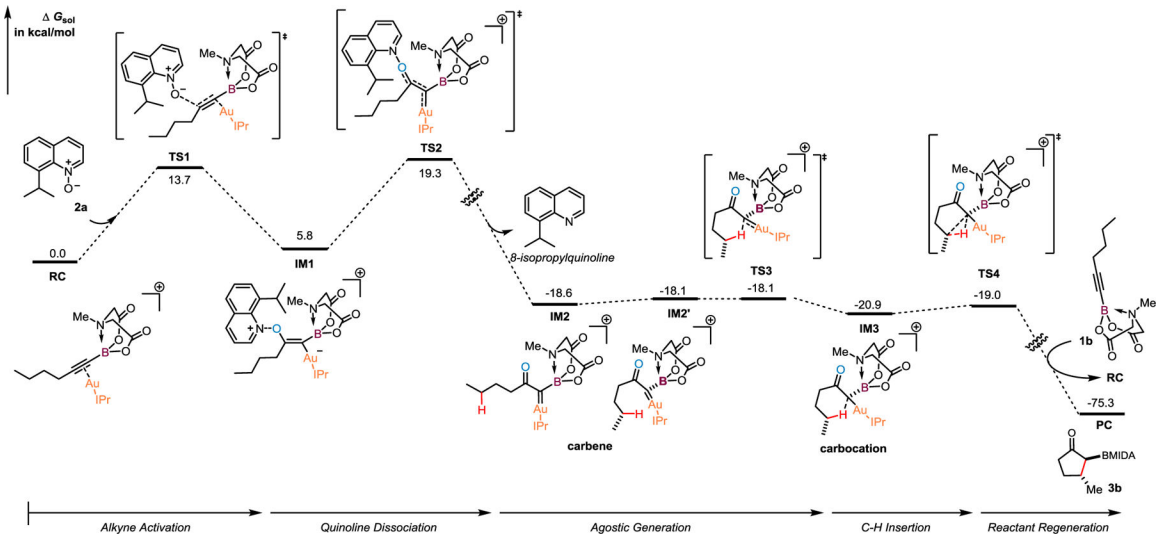

Figure 1.

The free energy profile of the Au-catalyzed oxidation of BMIDA alkyne **1b**.

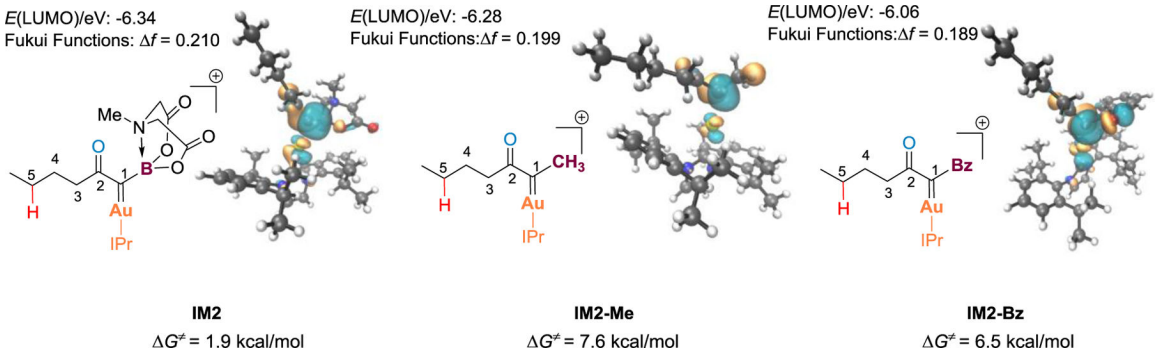

Figure 2.
LUMO (Isovalue = 0.03) and electronic parameters for the Au-carbene intermediates.

Author Manuscript Author Manuscript Author Manuscript Author Manuscript

Author Manuscript Author Manuscript Author Manuscript Author Manuscript

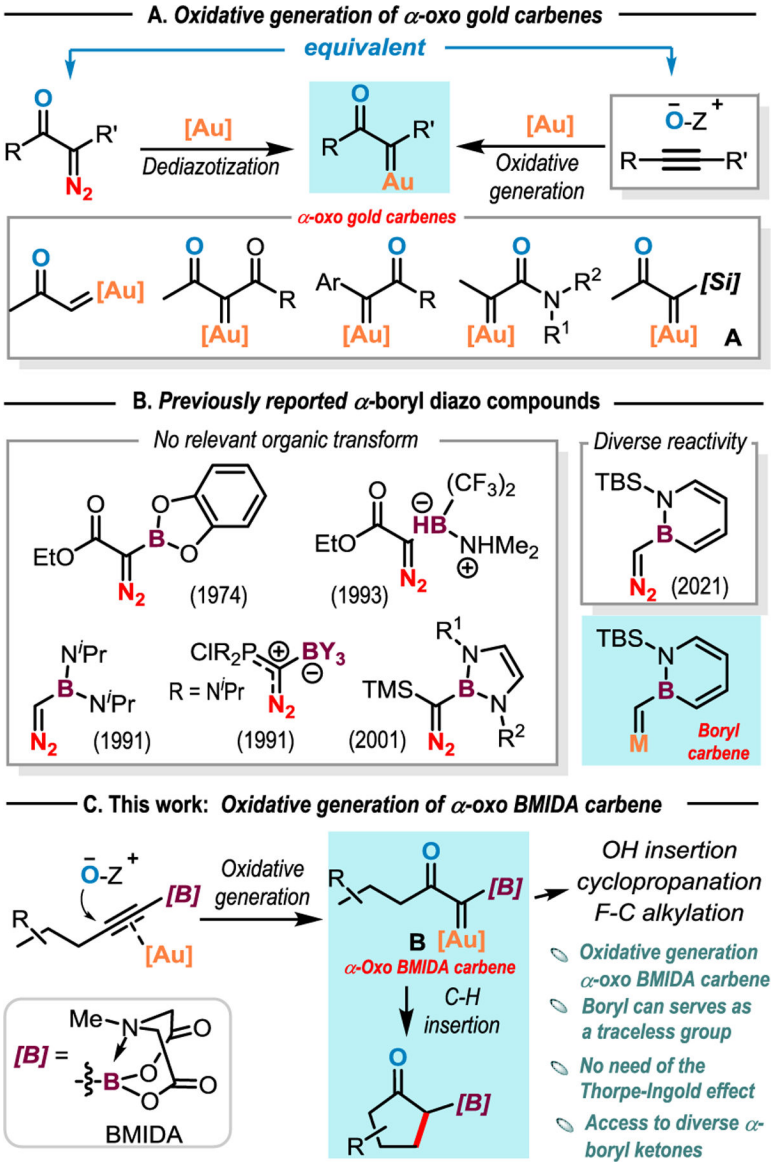

Scheme 1.

Generation of α-oxo boryl gold carbenes via gold-catalyzed alkyne oxidation.

Author Manuscript Author Manuscript Author Manuscript Author Manuscript

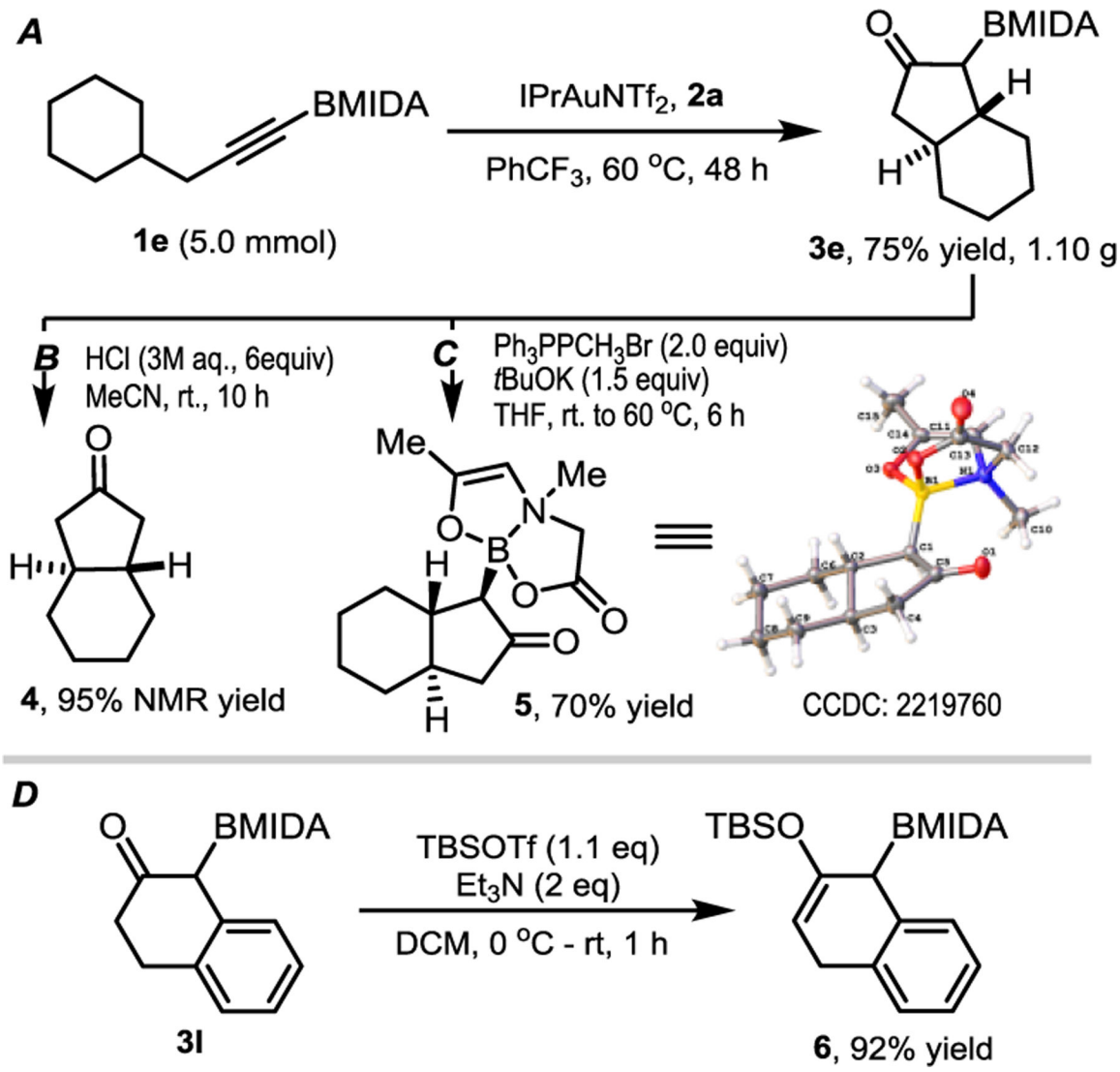

Scheme 2.
Gram-scale reaction and synthetic transformations.

Author Manuscript Author Manuscript Author Manuscript Author Manuscript

Table 1.

Reaction optimization.[a]

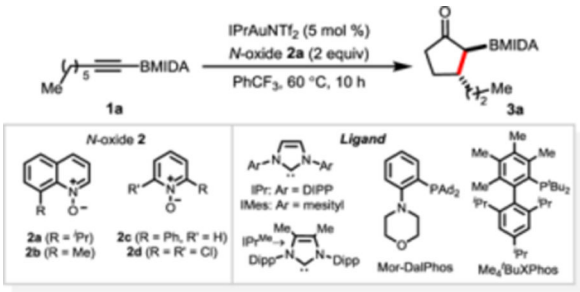

Entry	Deviation from the optimal reaction conditions	Yield[b]
1	none	85% (80%[c])
2	$IMesAuNTf_2$ instead of $IPrAuNTf_2$	73%
3	$IPr^{Me}AuCl/AgNTf_2$ instead of $IPrAuNTf_2$	65%
4	$Me_4{}^tBuXPhosAuCl/AgSbF_6$ instead of $IPrAuNTf_2$	trace[d]
5	$MorDalPhosAuNTf_2$ instead of $IPrAuNTf_2$	35[d]
6	$IPrAuCl/AgSbF_6$ instead of $IPrAuNTf_2$	72%
7	$AgNTf_2$ instead of $IPrAuNTf_2$	-
8	**2b** instead of **2a**	67%
9	**2c** instead of **2a**	0[d]
10	**2d** instead of **2a**	0[d]
11	DCE instead of $PhCF_3$	77
12	PhF instead of $PhCF_3$	79
13	toluene instead of $PhCF_3$	63
14	THF instead of $PhCF_3$	<4%[d]

[a]Initial [**1a**] = 0.033 M.

[b]NMR yields determined by using 1,3,5-trimethoxybenzene as internal reference. dr >20:1.

[c]Isolated yield.

[d]Most of the starting material **1a** was recovered. DCE: 1,2-dichloroethane; THF: tetrahydrofuran.

Author Manuscript Author Manuscript Author Manuscript Author Manuscript

Table 2.

The scope of insertion into C(sp^3)-H bonds.[a]

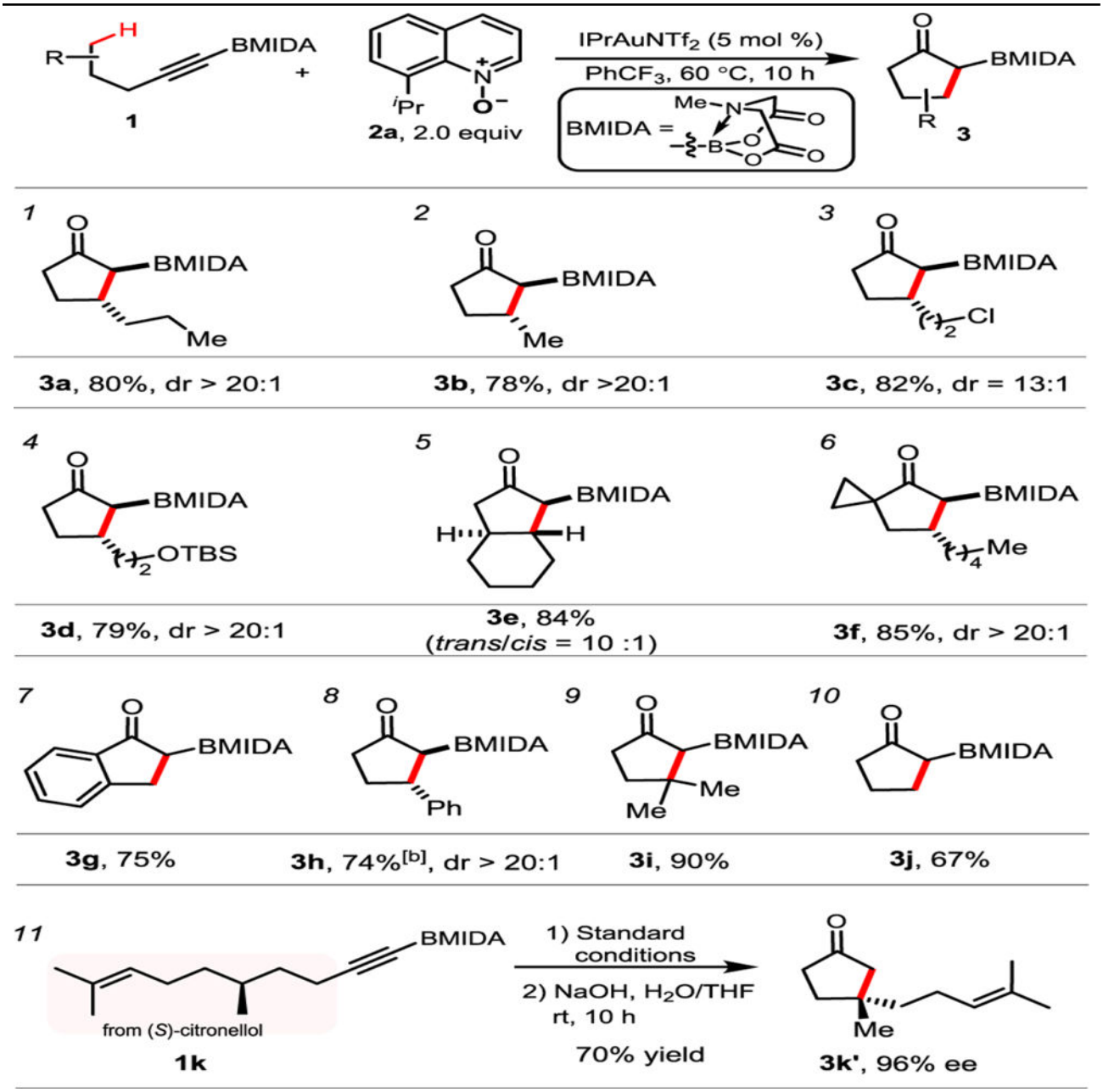

[a]Reaction conditions: **1** (0.15 mmol), **2a** (0.30 mmol), $IPrAuNTf_2$ (5 mol %) in $PhCF_3$ (2 mL) at 60 °C for 10 h. The d.r. value was determined by ^1H NMR.

[b]At 40 °C for 24 h.